PERSPECTIVE

Dalton
www.rsc.org/dalton

The active site and catalytic mechanism of NiFe hydrogenases †

Anne Volbeda and Juan C. Fontecilla-Camps *
Laboratoire de Cristallographie et de Cristallogenèse des Protéines, Institut de Biologie Structurale 'Jean-Pierre Ebel', CEA, CNRS, UJF. 41, rue Jules Horowitz, 38027 Grenoble Cedex 1, France. E-mail: juan@lccp.ibs.fr

Received 22nd April 2003, Accepted 2nd June 2003
First published as an Advance Article on the web 22nd September 2003

This Perspective describes, from our own personal experiences, how the architecture of the NiFe hydrogenase active site has been elucidated by a combination of protein crystallography, Electron paramagnetic resonance and Fourier transform infrared spectroscopic studies. Thus within a period of eight years our perception of the active center has changed from a mononuclear Ni center with S and N/O coordination to a binuclear NiFe unit with thiolate (to Ni and Fe) and CO and CN^- (to Fe) ligands. This biologically unusual organometallic cluster poses a real challenge in terms of understanding the role of its different components. Current ideas concerning the NiFe hydrogenase catalytic mechanism are discussed in this context.

1 Introduction

Although nickel, along with iron, is a major component of the Earth core and a combination of these two transition metals has been implicated as a central component in the "FeS" chemoautotrophic theory of the origin of life,[1] the former is much rarer than the latter in contemporary biological systems. In fact, Ni has only been described as being part of a few enzymatic systems.[2] Of these, four catalyze redox reactions that could be related to primordial processes and, remarkably, they all involve gases: H_2 in the case of NiFe-hydrogenases, CO and CO_2 in carbon monoxide dehydrogenase (CODH)/acetyl-Coenzyme A synthase (ACS) and CH_4 in methyl-Coenzyme M reductase.[3] It is therefore tempting to assume that, in spite of their perplexing complexity, these enzymes were essential in providing non-solar, chemically-generated, energy, as well as a carbon source, to primitive microorganisms at the early stages of life evolution on Earth. Potentially similar microbial communities subsisting indepently from solar energy have been described in some contemporary niches.[4]

For almost 10 years, we have been interested in the structural aspects of the catalytic role of Ni in hydrogen metabolism, and, much more recently, in the implication of this metal in CO_2 reduction and in the synthesis of acetyl-CoA,[5] a central molecule in many metabolic pathways. In this article, we will

† Based on the presentation given at Dalton Discussion No. 6, 9–11th September 2003, University of York, UK.

Anne Volbeda obtained his Ph. D. degree in 1988 at the University of Groningen after working with Wim Hol on the crystallographic analysis of spiny lobster haemocyanin, a large hexameric protein that uses binuclear copper centres to transport molecular oxygen. During a post-doctoral fellowship with Dietrich Suck at EMBL Heidelberg he worked on the crystal structure of P1 nuclease, an enzyme with a trinuclear zinc active site. In 1991 he obtained a permanent position at the laboratory of crystallography and crystallogenesis of proteins (LCCP) in Grenoble, where he continued doing research on the structure and function of complex redox enzymes depending on iron and nickel. His main themes of interest focus on electron, proton and gas transfer phenomena in proteins and on the functioning of metal sites in biochemical energy transformations.

Juan C. Fontecilla-Camps got his undergraduate training at the University of Concepcion, Chile, and his Ph. D. degree in protein crystallography at the University of Alabama in Birmingham under the supervision of Charles E. Bugg in 1980. Subsequently, he moved to Marseilles, France, where he became group leader and then head of a protein crystallography laboratory established by the CNRS and the University of Aix-Marseilles. In 1991, he took a job with the French Commissariat à l'Energie Atomique (CEA) in Grenoble. After having worked on the crystal structure of animal toxins, in 1993 he turned his attention to the structural biology of hydrogenases and other metalloenzymes. He and his group have solved the structures of NiFe and Fe-only hydrogenases, pyruvate–ferredoxin oxidoreductase and, very recently, carbon monoxide dehydrogenase/acetyl-Coenzyme A synthase. In 2000, he was awarded the medal of the European section of the International Society of Biological Inorganic Chemistry for his work on hydrogenases. He is also "Chevalier dans l'Ordre des Palmes Académiques" of the French Republic.

Anne Volbeda

Juan C. Fontecilla-Camps

DOI: 10.1039/b304316a

comment on how protein crystallography has contributed to elucidating the active site structure of NiFe hydrogenases and how, along with available spectroscopic and biochemical data, it has allowed us and others to propose plausible catalytic mechanisms for these enzymes.

2 What was know about NiFe hydrogenases before the crystallographic analysis

Hydrogenases, a class of enzymes present in microorganisms capable of using hydrogen as a nutrient or protons as electron acceptors, were first described in 1931 by Stephenson and Stickland.[6] It was subsequently found that at least some hydrogenases are Ni-containing enzymes, as shown by electron paramagnetic resonance (EPR) spectroscopic studies using ^{61}Ni-substituted *D. gigas* hydrogenase.[7] Amino acid sequence analyses indicated the presence of several cysteine-containing conserved motifs that were assigned to three FeS clusters contained in the small subunit and the active site present in the large subunit.[8] The latter consisted of two pairs of cysteines found near the N- and C-termini, respectively. Furthermore, both X-ray absorption spectroscopy (XAS) and EPR studies showed that a unique selenocysteine, that replaces one of the invariant cysteines in the C-terminal region of a few hydrogenases, was a Ni ligand.[9] Additional EXAFS experiments suggested that the active site of these enzymes was a mononuclear Ni center with a mixed S and N/O coordination.[10] When the enzyme was purified in the presence of air, two different Ni EPR spectra were observed. They were denoted Ni–A and Ni–B and showed very different behaviors upon reductive activation of the hydrogenase.[11] The Ni–A state has also been denoted "unready" because it requires relatively high temperatures and a significant lag time to activate. The Ni–B form, on the other hand, has been denoted «ready» because it activates very quickly. Both oxidized forms are thought to correspond to Ni(III). Another paramagnet is obtained when the enzyme is partially reduced under hydrogen and this species, generally considered to be a catalytic intermediate state, is denoted Ni–C.[12] Ni–C can be photolysed giving rise to additional EPR signals that have been assigned, using D/H isotopic exchange, to changes in hydron (H^+, H or H^-) binding to the active site induced by light.[13] In addition to these EPR-active forms, NiFe hydrogenases can be obtained in two diamagnetic forms denoted Ni–SI and Ni–R which are also thought to be catalytically relevant. Redox titrations performed by Paul Lindahl and coworkers have indicated that the sequence Ni–SI $\longrightarrow$ Ni–C $\longrightarrow$ Ni–R is most likely produced by successive one-electron reducing steps.[14]

EPR signals were also observed for the FeS clusters: the oxidized hydrogenase displayed a spectrum typical of a $[Fe_3S_4]^{1+}$ cluster that disappeared upon reduction which then produced a signal characteristic of $[Fe_4S_4]^{1+}$ clusters. From these EPR data, along with metal content determinations, it was concluded that the NiFe hydrogenase from *D. gigas* contained one $[Fe_3S_4]$ and two $[Fe_4S_4]$ clusters[15] that, based on the position of conserved cysteine residues in the amino acid sequence, were located in the small subunit.[8]

3 The crystal structure of NiFe hydrogenase from the sulfate-reducing bacterium *Desulfovibrio gigas*

In 1987 the crystallization of two NiFe hydrogenases were reported, both from sulfate-reducing bacteria: *D. vulgaris* Miyazaki F and *D. gigas*.[16] More suitable crystals of the latter were subsequently obtained in our laboratory by refining conditions previously determined by Chantal Abergel, now at the CNRS, Marseilles. The very best crystals of *D. gigas* hydrogenase ever grown by us came from the initial batches provided by E. Claude Hatchikian, also from CNRS, Marseilles. We were able to collect a 2.85 Å resolution native room-temperature data set from six crystals using Cu-Kα radiation from a rotating anode generator and an area detector in our laboratory and from one additional crystal at the French synchrotron at Orsay (Laboratoire Universitaire de Rayonnement Electromagnetique). The structure was solved using the Multiple Isomorphous Replacement (MIR) method. We published an account of a preliminary 5 Å resolution analysis in the CCP4 Newsletter in 1993.[17] Both standard and anomalous difference electron density maps showed a neat arrangement of three strong peaks and a weaker one separated by about 12 Å from center to center, a distance typical for redox centers involved in electron transfer (Fig. 1). We assigned the weakest peak to the active site because, according to the available data, we expected it to be composed of a mononuclear Ni center. In those pre-European Synchrotron Radiation Facility (ESRF) days, we were less aware of the use of anomalous scattering to identify electron-rich scatterers; otherwise we would have realized that the active site peak we found in the anomalous difference map could not arise from Ni because Cu-Kα radiation (1.5418 Å) is on the *low* energy side of the Ni absorption edge (1.4881 Å).

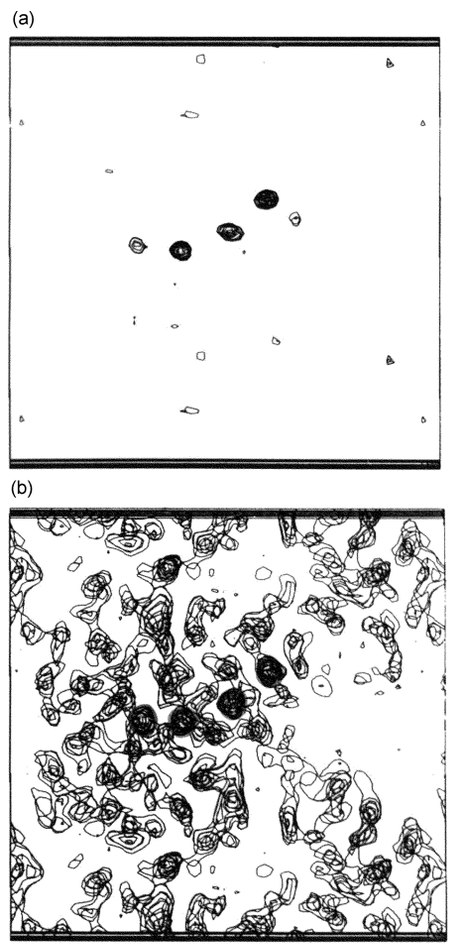

Fig. 1 Multiple isomorphous replacement phased maps of *D. gigas* NiFe hydrogenase at 5 Å resolution, showing a slab of the electron density. (A) Anomalous difference map, contoured at multiples of 1σ (the root mean square level of the map), with starting level of 3σ. (B) Solvent flattened electron density map, also at multiples of 1σ. The highest density features in both maps were assigned to four metal sites, from right to left: $[Fe_4S_4]$, $[Fe_3S_4]$, $[Fe_4S_4]$ and the Ni-containing active site.[17]

Eventually, we obtained an atomic model from a 2.85 Å electron density map (Fig. 2).[18] Two major unexpected features were evident from this map:

(1) The tracing of the polypeptide chain could not be extended beyond His536 (Fig. 3), fifteen residues away from the

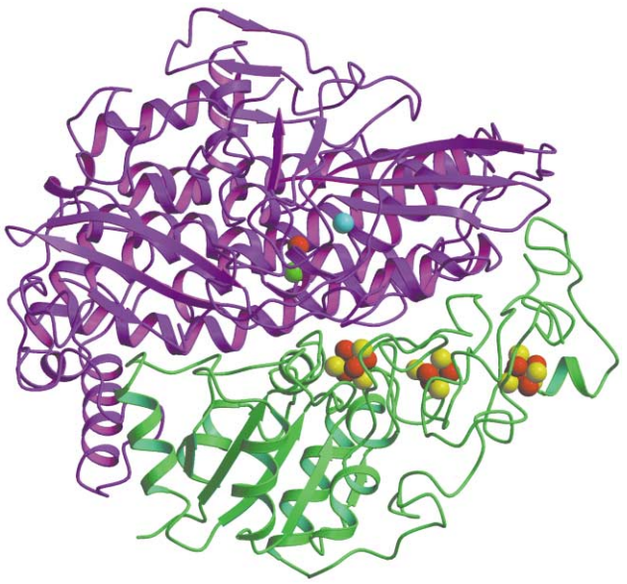

Fig. 2 Polypeptide fold of *D. gigas* NiFe hydrogenase. The small and the large subunit are depicted in green and purple, respectively, using ribbons for α-helices and arrows for β-strands. Metals and inorganic sulfur atoms are depicted as spheres, showing the presence of three iron–sulfur clusters in the small subunit and of three metal ions in the large subunit. Of these, the nickel (in green) is situated closest to the center of the heterodimeric structure.

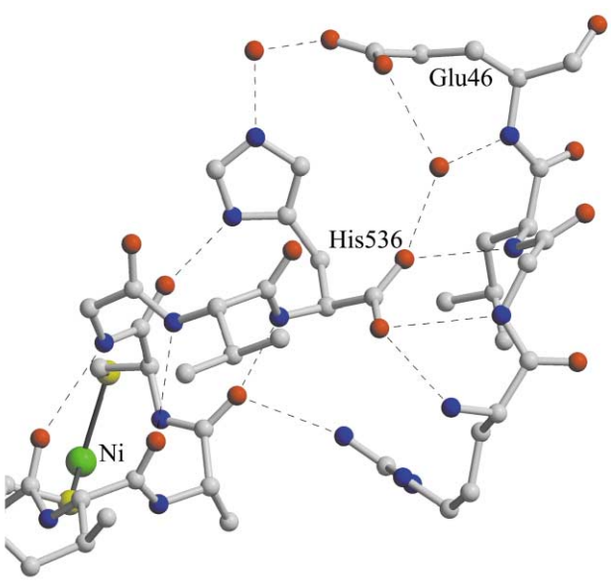

Fig. 3 Structure of the C-terminal region of the large *D. gigas* NiFe hydrogenase subunit, showing putative H-bonding interactions as dashed lines. Used color codes: C (gray), S (yellow), O (red), Ni (green) and N (blue). The imidazole side chain of the C-terminal His536 and the carboxylate group of Glu46 are bonded to an atom that was initially assigned as a water molecule, but which later turned out to be a Mg^{2+} ion. The Ni is shown bonded to two of the four thiolate ligands.

C-terminal Leu551, according to the gene sequence. This was particularly disquieting because His536 is deeply buried in the structure and, consequently, the absence of electron density for the C-terminal fifteen residues could not be assigned to disorder due to exposure to the solvent medium. Fortunately, we then found out that a recent report had described the maturation process in hydrogenases as consisting of the cleavage of a C-terminal polypeptide followed by assembly of the Ni-containing active site.[19] From the relative positions of the active site and the C-terminal His536 it was easy to postulate a re-organization of the large hydrogenase subunit upon cleavage including internalization of the Ni ion.

(2) The Fourier map at the active site displayed excessive electron density for a mononuclear Ni site. It was easy to identify the Ni ion because we knew that Cys530 was one of its ligands from the SeCys EPR and XAS experiments mentioned above.[9] Crystallographic refinement of the hydrogenase model at 2.85 Å resolution indicated that the extra electron density could be interpreted as an additional metal center X bound to three non-proteinacious small molecules. These were modelled as water although it was clear that their identity remained to be determined (Fig. 4).[18]

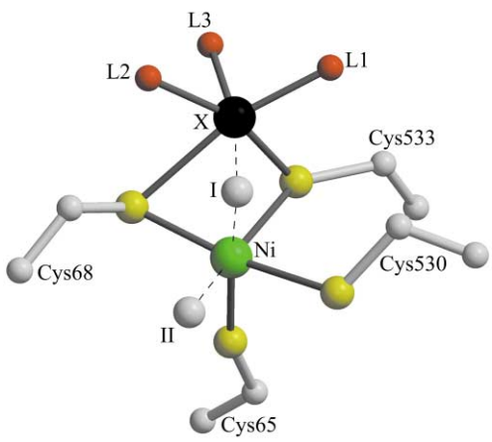

Fig. 4 Active site structure based on a first 2.85 Å resolution crystallographic analysis.[18] No significant electron density was found for the two Ni coordination sites (depicted as gray spheres) that are labelled I and II. These sites could bind substrate. Site I is also within bonding distance of metal X. The Ni is bound by four cysteine residues, two of which bind also to metal X, which further binds three small ligands (L1, L2 and L3) that were initially modelled as water molecules.[18]

4 Towards a higher resolution model of the active site

So far, mostly rotating anode generator room temperature data had been collected from *D. gigas* hydrogenase crystals. Then, in 1996 it became possible to use the very intense X-ray source of the ESRF. Using this synchrotron radiation, however, required the development of cryocrystallographic techniques in order to protect the crystals from radiation damage. In addition, the use of cryogenic temperatures prevented oxidative damage by air, which previously had limited the useful lifetime of hydrogenase crystals kept at room temperature to only one or two days. Although the now classical approach of flash-cooling a crystal mounted in a loop using a 100 K N_2 gas stream worked fine for the oxidized hydrogenase, new techniques to flash-cool crystals within a glove box were necessary to stabilize reduced forms of the enzyme, as indicated below.[20] Although by this time our crystals were not nearly as good as the initial ones, it was possible to collect data at 100 K to 2.54 Å resolution from one very thin needle-like crystal at the ESRF with the help of Bjarne Rasmussen. This new crystal form was very advantageous because it contained six independent molecules in the asymmetric unit (against only two in the initial crystals). Electron density averaging over the corresponding six equivalent regions produced an excellent map where new features could be identified at the active site: a small peak located between Ni and X and subsequently modelled as an oxo ligand and three elongated features coming out X, where water had been previously included (Fig. 5).[21] At about the same time, Simon Albracht from Amsterdam University and Kimberly Bagley then at Los Alamos National Laboratory, had been studying the binding of CO, a potent inhibitor, to the NiFe hydrogenase from *Allochromatium vinosum* using Fourier transform infrared spectroscopy (FTIR). Triple-bonded molecules like CO display

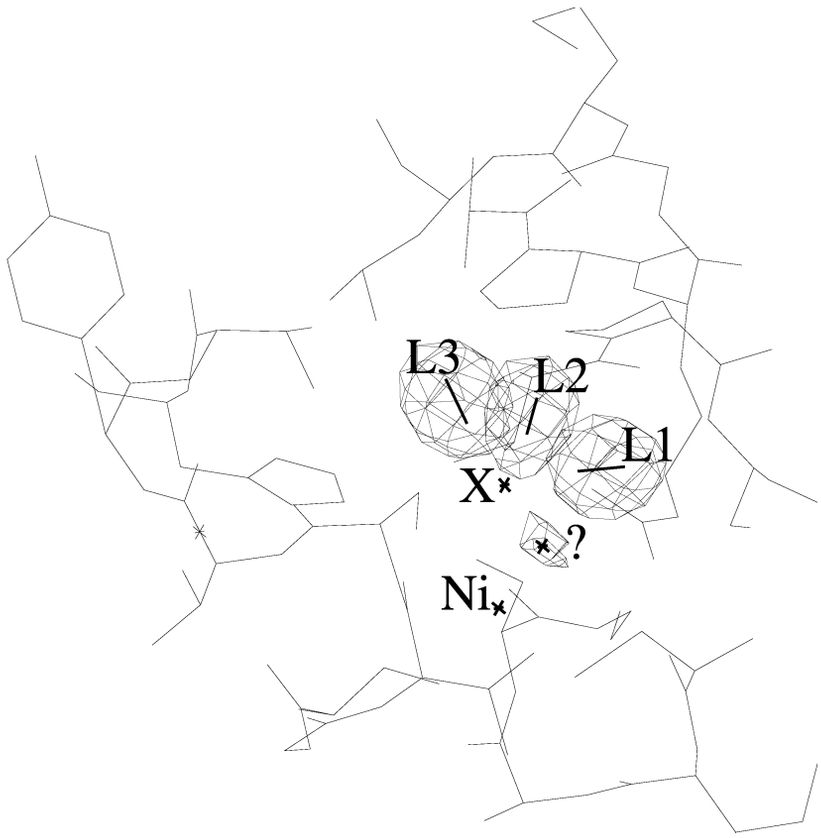

Fig. 5 Six-fold averaged $F_{obs} - F_{model}$ omit electron density map, shown as a fine grid, of a pseudo-hexagonal crystal form of *D. gigas* NiFe hydrogenase refined at 2.54 Å resolution.[21] Protein residues are shown with thin bonds. An electron density peak of a small bridging ligand is labelled with a question mark. Similar peaks were found for many ordered water molecules. The strong electron density found for the L1, L2 and L3 ligands of metal X indicated that these did not correspond to water. They were subsequently assigned as diatomic molecules with triple bonds that are known now to correspond to one CO and two CN^- ligands.[22]

frequency bands at about 1900–2000 cm^{-1}, a region where protein-based bands are generally absent. To their surprise, not only did they observe the band arising from the added CO but also three additional bands that were present even in the absence of exogenous CO. Subsequently, these authors carried out FTIR measurements on hydrogenase purified from cells grown in the presence of either $^{15}NH_3$ or $^{13}CO_2$. In the first case, they noticed that the two higher frequency bands shifted whereas the lower band remained unchanged; in the second case, all three bands shifted. From these studies, as well as chemical analyses using the denatured enzyme, Albracht and co-workers concluded that the three bands arised from one CO and two CN^- molecules.[22] With this information at hand, we showed that the ligands of X could be crystallographically modelled as diatomic molecules and that from the active site environment it was possible to distinguish CO from CN^-; the former sat in a hydrophobic pocket whereas the latter formed hydrogen bonds with protein atoms (Fig. 6).[23] The presence of the diatomic ligands made it possible to use FTIR to identify the various redox states, including those that are EPR-silent (see below).

At this point, the identity of X had not been definitively established. We had argued that it was probably Fe because metal content analyses of *D. gigas* hydrogenase have only reported Ni and Fe and, given the presence of three FeS clusters, the exact amount of the latter was not easy to determine. We solved this problem by collecting X-ray data at either side of the Fe absorption edge and then extracted the anomalous differences (Δ_{anom}) between Bijvoet pairs to calculate Fourier maps with Δ_{anom} coefficients. If X were Fe, then the map calculated at the low energy side (λ_1) of its edge should be featureless whereas the one calculated at the high energy side (λ_2) should contain a peak at the putative Fe center. A simple way of depicting these results is to calculate a double difference map by substracting the $\Delta_{anom}\lambda_1$ map from the $\Delta_{anom}\lambda_2$ map. This experiment showed unambiguously that X was indeed Fe and that, consequently, the hydrogenase active site consists of a NiFe dinuclear center (Fig. 7).[21]

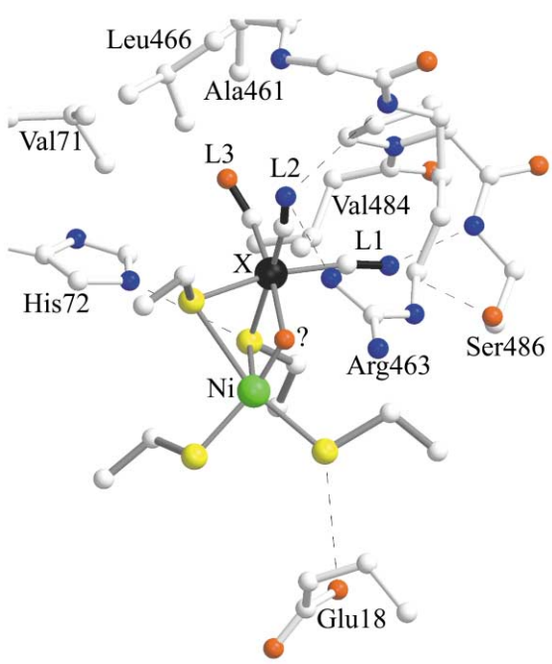

Fig. 6 Ball-and-stick representation of the protein environment of the active site, as found in the model refined at 2.54 Å resolution.[21] Dashed lines indicate putative H-bonding interactions, including those to L1 and L2. Only hydrophobic residues surround L3. Accordingly, L1 and L2 were assigned to the two CN^- anions and L3 to the neutral CO ligand.[23]

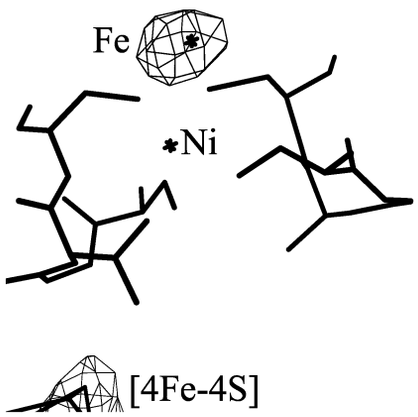

Fig. 7 Assignment of metal X to Fe by a 11.3σ peak in a double difference $\Delta_{anom}(\lambda = 1.733$ Å) − $\Delta_{anom}(\lambda = 1.750$ Å) map,[21] shown as a fine grid. The two used X-ray wavelengths (λ) correspond to the high and the low energy side of the Fe absorption edge.

This finding was surprising because the Fe center went undetected by XAS and other spectroscopic techniques. It has been argued that this situation was caused by long S–Ni bonds (that masked the Fe in XAS experiments)[24] and by the fact that the active site Fe is always low-spin Fe(II) (although a more recent account has confirmed the presence of an active site Fe using EPR).[25]

5 Hydrophobic channels

A remarkable feature of NiFe hydrogenase, and other gas-metabolizing enzymes such as CODH/ACS,[5] is the presence of hydrophobic channels that determine how gas substrates and products circulate inside the protein. In order to test the ability of these channels to bind gas, a crystal was mounted at room temperature in a glass capillary that was, in turn, connected to a pressurized Xe source. A 6 Å X-ray data set was collected under 9 bar of Xe pressure using a rotating anode generator and an area detector. Xe is a convenient gas because it is very electron-rich and, consequently, easy to visualize in Fourier maps. This study showed the presence of 10 peaks all contained within the hydrophobic channels. Subsequently, a total of 12 peaks were found in an difference electron density map calculated using a higher resolution data set measured at the ESRF from a flashed-cooled crystal (Fig. 8).[26] In order to better mimic the real situation, hydrogen molecules were placed at the experimentally observed Xe sites and a molecular dynamics study was carried out in collaboration with Patricia Amara and Martin Field of our Institute.[26] Two relevant observations were made: (1) during the simulation molecular hydrogen did not leave the hydrophobic channels while inside the protein and (2) some substrate molecules accessed the active site and then left the enzyme, confirming the assumption that the channels form a connection between the medium and the NiFe center. The first observation indicates that hydrogen diffusion through the protein matrix (as assumed prior to our work) does not occur. The second observation sheds light on the nature of the primary hydrogen binding site: the hydrophobic channel peters out near a vacant terminal Ni binding site. Its availability has been confirmed by the binding of the competitive inhibitor CO to this Ni site reported by Higuchi and co-workers.[27]

6 The active site of NiFe hydrogenase from *D. vulgaris* Miyazaki F

In 1997, Higuchi *et al.* published the structure of the closely-related *D. vulgaris* enzyme and reported two major differences with our results:[28] the bridging ligand was assigned to be S^{2-} and, more importantly, one of the diatomic ligands was modelled as SO. The presence of S^{2-} posed no special problem

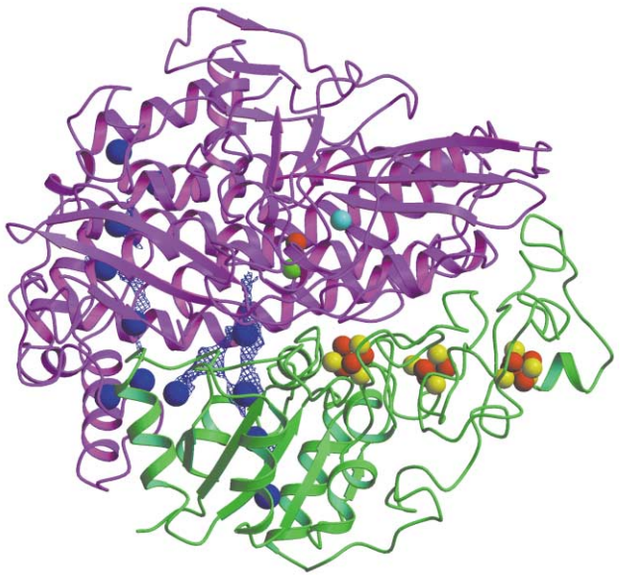

Fig. 8 Gas accessibility to the NiFe-hydrogenase active site. The dark grid shows an average accessibility map of the superimposed *D. gigas* and *Dm. baculatum* hydrogenase structures, indicating conserved hydrophobic cavities and channels. Twelve internal xenon sites, depicted as large black spheres, were found in gas binding experiments performed with *D. fructosovorans* NiFe-hydrogenase,[26] showing that these channels may function in providing H_2 access to the deeply buried active site. Color codes as in Fig. 2.

as this ligand was not intrinsic to the protein and could most likely exchange depending on the environment. The same could not be said for the buried SO because it would correspond to an active site Fe intrinsic ligand equivalent to CO or CN^-. In order to rationalize the presence of three high frequency bands (SO would not generate bands in the 1900–2000 cm^{-1} region) these authors invoked a constant SO but different combinations of CO and CN^- at the active site.[28] According to Higuchi *et al.*, further support for their proposition was obtained from pyrolytic experiments that were carried out on *D. vulgaris* hydrogenase and showed the evolution of SO-related compounds.[28] Curiously, we have not been able to identify a SO ligand to the active site Fe in any of the three different hydrogenases we have studied so far (see below). A more unified image has emerged with the recent report by Higuchi and co-workers of the structural study at 1.2 Å resolution of CO-inhibited *D. vulgaris* hydrogenase mentioned above where they did not detect SO at the NiFe active site. Instead, the correponding ligand was refined as CO.[27]

7 Exploring the catalytic mechanism by mutagenesis and the study of redox intermediates

Two aspects must be taken into account when studying catalysis by metalloenzymes: the role of the metal center, which can be mostly understood in terms of coordination and organometallic chemistry, and the influence of the protein environment in determining the properties of the active site as a whole, as well as modulating substrate and product circulation. Mutagenesis studies based on amino acid sequence and structural comparisons have been directed at the invariant thiolate ligands and have highlighted their critical role in coordinating the NiFe unit.[29]

Structure-inspired hydrogenase mutants

The molecular biology of NiFe hydrogenase from sulfate-reducing bacteria has been developed using *D. fructosovorans.*[30] For this reason we decided that it was necessary to carry out the crystallographic analysis of this hydrogenase also. After having solved the structure of the wild type enzyme and in collabor-

ation with Marc Rousset from CNRS, Marseilles, we determined the structures of two hydrogenase mutants. The first one consisted in the transformation of the [Fe_3S_4] median cluster (Fig. 9) into a [Fe_4S_4] cluster by the mutation of a proline residue into cysteine (this mutation was inspired by the presence of a Cys at that position in the *Desulfomicrobium baculatum* hydrogenase that was known to lack a [Fe_3S_4] cluster). Although the mutation shifted the redox potential of the medial cluster by more than −200 mV it had almost no effect in catalysis, suggesting that internal electron transfer is not the limiting step in the reaction.[31] The second mutation concerned a serine residue that forms a hydrogen bond with one of the CN^- ligands to the active site Fe center. We expected to see changes in the FTIR spectrum of this mutant. However, when replaced by alanine, the missing OH function was topologically substituted by a water molecule and the mutant enzyme displayed wild type-like catalytic properties and FTIR bands.[32,33]

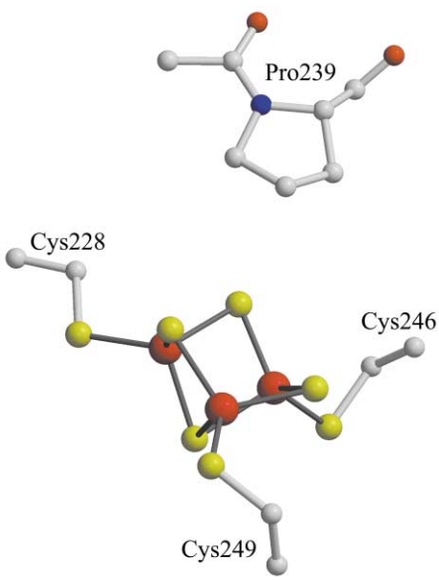

Fig. 9 Binding of the [Fe_3S_4] cluster to three Cys-ligands of the small subunit in *D. gigas* hydrogenase. The shown proline residue is substituted by a cysteine in the *Dm. baculatum* NiFeSe-hydrogenase, thus providing a binding site for a fourth Fe ion in this cluster.

Redox intermediates

The initial *D. gigas* hydrogenase structure was determined from as-prepared material and as shown by the EPR signals it contained a mixture of the oxidized forms: about 43% Ni–A, 7 % Ni–B and 50 % of EPR-silent hydrogenase molecules.[18] In order to get an image of the reduced active site we crystallized the NiFeSe enzyme from *Dm. baculatum*, known to be resistant to oxidation of the active site and not to display the Ni–A EPR signal. The crystals were exposed to 10 bars of hydrogen pressure for 30 min and then rapidly flash-cooled inside the glove box using a liquid propane-based technique developed in our laboratory.[20] Diffraction data at 2.15 Å resolution collected from one of these crystals showed that the reduced active site displayed several changes relative to the oxidized counterparts from *D. gigas* and *D. fructosovorans* previously studied. As expected, the selenium atom from the modified cysteine that is terminally bound to Ni was a strong feature in the electron density map. More interestingly however, the small NiFe bridging putative oxo ligand found in the oxidized enzymes was absent from this map and the distance between the two metals ions changed from 2.95 to 2.55 Å (Fig. 10). This shows that the putative oxo ligand is a signature of the oxidized active site.[34] At the same time, Higuchi *et al*. published the reduced structure of the *D. vulgaris* Miyazaki F enzyme with similar results: the S^{2-} bridging ligand reported in their oxidized enzyme was absent from the active site.[35] Although we do not know the exact oxidation state of our reduced crystals, it seems likely they were in a mixture of Ni–C and Ni–R states. These forms probably have bound hydrons but they cannot be detected by protein crystallographic techniques at the available resolutions.

Table 1 IR frequencies (cm^{-1}) of active site redox states in *D. gigas* NiFe hydrogenase[21]

Redox state	Band 1 (CO)	Band 2 (CN^-)	Band 3 (CN^-)
Ni–A	1947	2083	2093
Ni–B	1946	2079	2090
Ni–SU	1950	2089	2099
$Ni–SI_I$	1914	2055	2069
$Ni–SI_{II}$	1934	2075	2086
Ni–C	1952	2073	2086
Ni–R	1940	2060	2073

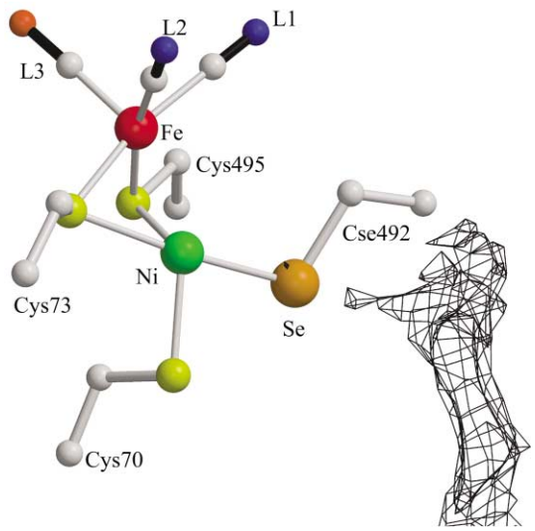

Fig. 10 Active site structure of a reduced form of the NiFeSe hydrogenase of *Dm. baculatum*, refined at 2.15 Å resolution.[34] Only four ligands to the Ni are visible in the electron density map, but an additional hydron Ni–Fe bridging ligand opposite to L3 may be present as well. As in other NiFe-hydrogenases, L1 and L2 are involved in H-bonding interactions with the protein environment and therefore are assigned to CN^-, whereas L3 most likely corresponds to CO as it is surrounded only by hydrophobic residues. A cavity map depicted as a black grid shows that H_2 may bind Ni at a vacant coordination site opposite to Cys495.

8 The use of FTIR to characterize NiFe hydrogenase redox states

Since the active site CO and, to a lesser extent, CN^- ligands have π-acceptor capabilities, they are able to take up electron density from the Fe center and stabilize it in a low oxidation state, most probable as Fe(II). In addition, the strong ligand field will favor low-spin, (S = 0) Fe. Changes in the oxidation state of the hydrogenase active site will affect the electron density sensed by the Fe ion and vary the degree of its back-donation to the diatomic ligands which, in turn, will change the order of the Fe–C and triple bonds. Controlled electrochemical titrations coupled to FTIR measurements have been performed by Albracht and co-workers[22] and by Fernandez and co-workers[23] from Madrid (Table 1). Because this technique does not depend on the magnetic state of the active site, it can detect both paramagnetic and diamagnetic forms. Thus besides the oxidized Ni–A/B and reduced Ni–C species, additional states have been spectroscopically identified using FTIR: Ni–SU, which is a putative Ni(II) unready species derived from Ni–A; two forms of Ni–SI differing by one proton and the more reduced Ni–R state (Scheme 1).[22,23]

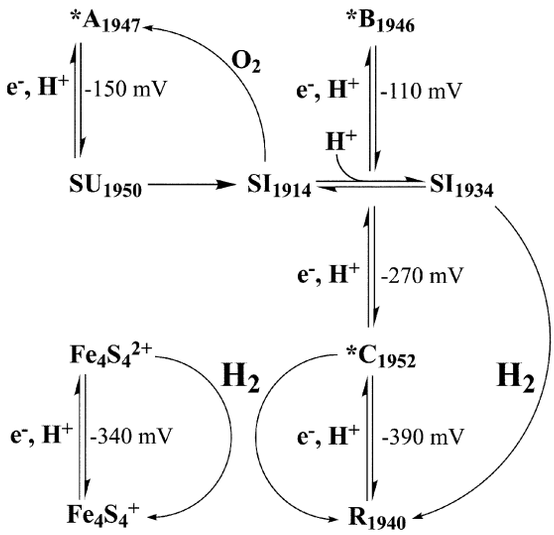

$$Fe_4S_4^{2+} + C_{1952} + H_2 \rightleftharpoons Fe_4S_4^{+} + H^+ + R_{1940}$$

$$SI_{1934} + H_2 \longrightarrow R_{1940}$$

Scheme 1

It is remarkable that the redox titration curves for the various active site states of *D. gigas* hydrogenase monitored by EPR and those followed by FTIR have the same shape.[36] This confirms the prediction of theoretical calculations that spin changes occur mostly at the Ni center whereas charge changes get delocalized over the active site and therefore are sensed by the Fe diatomic ligands.[37]

9 A comparison between NiFe and Fe-only hydrogenases

Besides the NiFe enzymes, there is another class of hydrogen metabolizing metalloproteins denoted as Fe-only hydrogenases.[38] The two classes are completely unrelated and consequently any common feature in their respective active sites may be considered as resulting from convergent evolution and therefore important for hydrogen catalysis. For instance, Fe-only hydrogenases are the only other metalloenzymes for which endogenous high frequency bands were detected using FTIR.[39] In 1998–1999 and within a period of two months the crystal structures of Fe-only hydrogenases from *Clostridium pasteurianum* and *D. desulfuricans* were reported.[40] The active sites of the two enzymes presented a few differences that resulted from interpretation and oxidation state rather than from real dissimilarities. Each of the two Fe ions present in the active site is coordinated by one terminal CO, one terminal CN^-, a bridging CO and two bridging thiolates from a small molecule thought to be di(thiomethyl)amine. In addition, one of the active site Fe ions has a vacant site and the other binds the thiolate from a Cys residue that is also bound to one of the Fe of a standard [Fe_4S_4] cluster. Peters and co-workers have shown that exogenous CO binds to the vacant Fe site of the *C. pasteurianum* active site, suggesting that this is the primary hydrogen binding site and may be involved in catalysis.[41] Work from our laboratory has demonstrated that the same Fe faces a short hydrophobic channel connecting the active center to the molecular surface.[40]

Upon reduction of the *D. desulfuricans* hydrogenase with molecular hydrogen, the active site bridging CO ligand forms a terminal bond with the putatively catalytic Fe. The overall coordination of this Fe is very similar to the one of the active site Fe of the FeNi *D. gigas* hydrogenase (Fig. 11) suggesting that

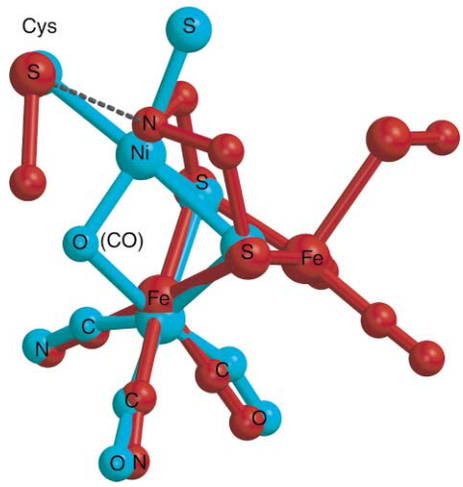

Fig. 11 Superposition of the active sites of NiFe (blue) and Fe-only hydrogenases.[42] Note the similar coordination sphere of the Fe ion in the former and one of the two Fe atoms in the latter. The dashed line shows a possible hydrogen bond (3.1 Å) between the central N atom of the putative di(thiomethyl)amine and the S_γ from Cys178. (CO) shows the position of this inhibitor according to Peters and co-workers.[41]

the catalytic mechanisms of the two classes of enzymes is similar and that Fe may be involved in hydride binding in both cases.[42]

10 Current ideas concerning the catalytic mechanism of NiFe hydrogenases

Hypotheses addressing plausible mechanisms of hydrogen metabolism by NiFe hydrogenases must explain the role of the different active site components, the function of the protein environment and integrate the known structural data. Although the Ni–A and Ni–B forms have attracted considerable attention over the years, they are not part of the catalytic cycle and their interest resides in their reversibility from oxygen-induced damage. (Other redox proteins from sulfate-reducing bacteria can also be reactivated by reduction, such as Fe-only hydrogenases,[38] or are inherently resistant to oxygen, such as the pyruvate–ferredoxin oxidoreductase from *D. africanus*[43]). Starting from one of the Ni–SI silent active forms, most likely a Ni(II) species with a vacant NiFe bridging site, molecular hydrogen is thought to diffuse from the medium to the active site through the hydrophobic channel and first bind terminally to Ni (Fig. 10). This assumption is reinforced by the fact that extrinsic CO, a competitive inhibitor of molecular hydrogen, has been shown to bind to Ni at that position.[27] What happens to the substrate after this step, which should generate the Ni–R state, has not been clearly established. One possibility is that hydrogen gets heterolytically cleaved between Ni and the terminal Cys530 (*D. gigas* numbering), the proton then gets transferred to the neighbouring Glu18 (Fig. 6). Support for a direct involvement of the terminal cysteine and the neighbouring glutamate in proton transfer comes from the fact that these moieties, along with the Ni ion, generally display higher-than-average temperature factors in our crystals, indicating a certain degree of disorder.[34] Such disorder could arise from various degrees of protonation/deprotonation of the cysteine and glutamate side chains. Indeed, the crystal structure of the NiFe hydrogenase from *D. desulfuricans* shows three different conformations for the equivalent cysteine residue.[44]

A second postulate, based on a rather simple model obtained from DFT calculations, assigns the catalytic hydrogen binding site to the Fe center.[45] This is attractive because of the similarity to the catalytic Fe in Fe-only hydrogenases (see above). After electron transfer to the proximal [Fe_4S_4] cluster, heterolytic cleavage occurs by proton transfer to Cys530, and the resulting hydride binds to the NiFe centre, probably bridging the two

metal ions in the Ni–C form. The cycle is closed by the transfer of one proton and one electron from the active site and the regeneration of the Ni–SI species (see Scheme 1). Because these DFT calculations did not take the protein environment into account, some of the obtained active site models deviate considerably from the crystallographically observed structures, thus casting doubts on the validity of the drawn conclusions for the actual enzyme. A third possibility is based on reports of hydrogen binding and cleavage by the Ni–C species,[14,46] which may already contain a bound hydride. This process would formally generate an undetectable state that is one electron more reduced than Ni–R. Hydrogen cleavage would then occur in this (transient) state, followed by transfer of one electron to the proximal $[Fe_4S_4]$ cluster, generating Ni–R. Here there would be no need to involve a Ni–SI state in the cycle. In conclusion, it is still under debate whether the catalytic hydrogen cleavage takes place in Ni–R, in a one-electron more oxidized or in a one-electron more reduced state.

11 Hydrogen as a fuel

Both environmental and strategic concerns have generated an increasing interest in hydrogen as a clean, potentially renewable energy source. Hydrogenase studies may contribute to the biotechnology of both hydrogen production and oxidation: there are ongoing efforts to couple photosynthesis, which uses solar energy, to hydrogen bioproduction. Many photosynthetic algae use hydrogenase to get rid of low-potential electrons through the reduction of protons.[47] One major problem with associating photosynthesis to hydrogenase activity is the high sensitivity of the enzyme to oxygen, a by-product of the water-splitting reaction. A possible solution to this problem could be to reduce the width of the hydrogenase hydrophobic channels mentioned above using site-directed mutaganesis in order to render them more selective to hydrogen than to oxygen. There is some evidence that the few oxygen-resistant hydrogenases such as the hydrogen-sensor proteins may have narrower hydrophobic channels.[32]

As far as hydrogen oxidation is concerned, recent elegant experiments using a hydrogenase-coated electrode have shown that the enzyme can be as effective as Pt in catalyzing that reaction.[48] The problem, of course, is the relative fragility of protein molecules when compared to inorganic catalysts. One way to circumvent this situation would be to synthesize small biomimetic molecules based on the active site of hydrogenases. For instance, the presence of $Fe(CO)_n(CN)_n$ (n = 1 or 2) units like the ones observed in both NiFe and Fe-only hydrogenases (Fig. 11) suggests that these low-spin Fe ions mimic lower row transition metals such as Pt and Ru, known to be good hydrogen catalysts (although in this case the cleavage is homolytic). The economic impact of substituting Pt by Fe as a catalyst for fuel cells would be enormous. Indeed, it has been argued that the global Pt production could not satisfy the demand if all the gasoline-propelled vehicles were to be replaced by hydrogen-operated ones.[49]

Unfortunately, and in spite of the significant efforts being made in several laboratories,[50] no biomimetic small molecule with catalytic properties that could be used in fuel cells has yet been synthesized.

12 Conclusions

In this Perspective, we have looked into the progress made in the last few years in understanding the way hydrogen is produced and oxidized by NiFe hydrogenases. As structural biologists, we have focused on the impact that determining the active site structure has had in our understanding of this process. We realize that many fundamental studies such as electron nuclear double resonance (ENDOR) and Mössbauer spectroscopic analyses;[51] EPR studies on oriented NiFe hydrogenase crystals,[52] Density functional theory calculations[53] and the elucidation of the fascinating genetic machinery that puts together the $NiFeCO(CN^-)_2$ unit,[54] have only been briefly mentioned, or not discussed at all. These studies are an integral and very important part of the hydrogenase field and their omission here has been only dictated by our preference to discuss those aspects for which we are more familair and have been more directly involved.

With the depletion of oil and natural gas sources, the use of hydrogen as a fuel in a more or less foreseeable future seems unavoidable. The question is whether any of the data coming from studying hydrogenases will be useful in either designing fuel cell catalysts or in improving hydrogen production from the biomass and from solar energy. We certainly hope that it will be the case.

Acknowledgements

We thank Claudine Darnault, Lydie Martin, Christine Cavazza, Yvain Nicolet, Yaël Montet, Elsa Garcin, Michel Frey, Victor M. Fernandez, E. Claude Hatchikian and Marie-Helene Charon for their essential contributions to our studies on the structural biology of hydrogenases.

References

1 (*a*) C. Huber and G. Wächterhäuser, *Science*, 1997, **276**, 245–247; (*b*) C. Huber and G. Wächterhäuser, *Science*, 1998, **281**, 670–673.
2 R. K. Watt and P. W. Ludden, *Cell. Mol. Life Sci.*, 1999, **56**, 604–625.
3 (*a*) S. W. Ragsdale, *Curr. Opin. Chem. Biol.*, 1998, **2**, 208–215; (*b*) R. P. Hausinger, *Microbiol. Rev.*, 1987, **51**, 22–42; (*c*) U. Ermler, W. Grabarse, S. Shima, M. Goubeaud and R. K. Thauer, *Curr. Opin. Struct. Biol.*, 1998, **8**, 749–758.
4 (*a*) A. Treiman, A. Wallendahl, D. R. Lovley, R. T. Anderson and F. H. Chapelle, *Science*, 1998, **282**, 2194; (*b*) Richard and A. Kerr, *Science*, 2002, **296**, 1056–1058.
5 C. Darnault, A. Volbeda, E. J. Kim, P. Legrand, X. Vernede, P. A. Lindahl and J. C. Fontecilla-Camps, *Nat. Struct. Biol.*, 2003, **10**, 271–279.
6 M. Stephenson and L. H. Stickland, *Biochem. J. (London)*, 1931, **25**, 205.
7 J. J. Moura, I. Moura, B. H. Huynh, H. J. Kruger, M. Teixeira, R. C. DuVarney, D. V. DerVartanian, A. V. Xavier, H. D. Peck, Jr. and J. LeGall, *Biochem. Biophys. Res. Commun.*, 1982, **108**, 1388–1393.
8 S. P. J. Albracht, *Biochim. Biophys. Acta*, 1994, **1188**, 167–204.
9 (*a*) M. K. Eidsness, R. A. Scott, B. C. Prickril, D. V. DerVartanian, J. Legall, I. Moura, J. J. Moura and H. D. Peck, Jr., *Proc. Natl. Acad. Sci. USA.*, 1989, **86**, 147–151; (*b*) S. H. He, M. Teixeira, J. LeGall, D. S. Patil, I. Moura, J. J. Moura, D. V. DerVartanian, B. H. Huynh and H. D. Peck, Jr., *J. Biol. Chem.*, 1989, **264**, 2678–2682.
10 M. J. Maroney, G. J. Colpas, C. Bagyinka, N. Baidya and P. K. Mascharak, *J. Am. Chem. Soc.*, 1991, **113**, 3962–3972.
11 R. Cammack, V. M. Fernandez and E. C. Hatchikian, *Methods Enzymol.*, 1994, **243**, 43–68.
12 M. Teixeira, I. Moura, A. V. Xavier, J. J. Moura, J. LeGall, D. V. DerVartanian, H. D. Peck, Jr. and B. H. Huynh, *J. Biol. Chem.*, 1989, **264**, 16435–16450.
13 (*a*) J. W. van der Zwaan, S. P. J. Albracht, R. D. Fontijn and E. C. Slater, *FEBS Lett.*, 1985, **179**, 271–277; (*b*) R. Cammack, D. S. Patil, E. C. Hatchikian and V. M. Fernandez, *Biochem. Biophys. Acta*, 1987, **912**, 98–109.
14 (*a*) D. P. Barondeau, L. M. Roberts and P. A. Lindahl, *J. Am. Chem. Soc.*, 1994, **116**, 3442–3448; (*b*) L. M. Roberts and P. A. Lindahl, *Biochemistry*, 1994, **33**, 14339–14350.
15 B. H. Huynh, D. S. Patil, I. Moura, M. Teixeira, J. J. Moura, D. V. DerVartanian, M. H. Czechowski, B. C. Prickril, H. D. Peck, Jr. and J. LeGall, *J. Biol. Chem.*, 1987, **262**, 795–800.
16 (*a*) Y. Higuchi, N. Yasuoka, M. Kakudo, Y. Katsube, T. Yagi and H. Inokuchi, *J. Biol. Chem.*, 1987, **262**, 2823–2825; (*b*) V. Niviere, C. Hatchikian, C. Cambillau and M. Frey, *J. Mol. Biol.*, 1987, **195**, 969–971.
17 A. Volbeda, C. Piras, M. H. Charon, E. C. Hatchikian, M. Frey and J. C. Fontecilla-Camps, *ESF/CCP4 Newslett.*, 1993, **28**, 30–33.
18 A. Volbeda, M. H. Charon, C. Piras, E. C. Hatchikian, M. Frey and J. C. Fontecilla-Camps, *Nature*, 1995, **373**, 580–587.

19 N. K. Menon, J. Robbins, M. Der Vartanian, D. Patil, H. D. Peck, Jr., A. L. Menon, R. L. Robson and A. E. Przybyla, *FEBS Lett*, 1993, **331**, 91–95.
20 X. Vernède and J. C. Fontecilla-Camps, *J. Appl. Crystallogr.*, 1999, **32**, 505–509.
21 A. Volbeda, E. Garcin, C. Piras, A. I. de Lacey, V. M. Fernandez, E. C. Hatchikian, M. Frey and J. C. Fontecilla-Camps, *J. Am. Chem. Soc.*, 1996, **118**, 12989–12996.
22 (*a*) K. A. Bagley, C. J. Van Garderen, M. Chen, E. C. Duin, S. P. Albracht and W. H. Woodruff, *Biochemistry*, 1994, **33**, 9229–9236; (*b*) K. A. Bagley, E. C. Duin, W. Roseboom, S. P. Albracht and W. H. Woodruff, *Biochemistry*, 1995, **34**, 5527–5535; (*c*) R. P. Happe, W. Roseboom, A. J. Pierik, S. P. Albracht and K. A. Bagley, *Nature*, 1997, **385**, 126; (*d*) A. J. Pierik, W. Roseboom, R. P. Happe, K. A. Bagley and S. P. Albracht, *J. Biol. Chem.*, 1999, **274**, 3331–3337.
23 A. L. De Lacey, E. C. Hatchikian, A. Volbeda, M. Frey, J. C. Fontecilla-Camps and V. M. Fernandez 1997, *J. Am. Chem. Soc.*, 1997, **119**, 7181–7189.
24 Z. Gu, J. Dong, C. B. Allan, S. B. Choudhury, R. Franco, J. J. G. Moura, I. Moura, J. LeGall, A. E. Przybyla, W. Roseboom, S. P. J. Albracht, M. J. Axley, R. A. Scott and M. J. Maroney, *J. Am. Chem. Soc.*, 1996, **118**, 11155–11165.
25 J. E. Huyett, M. Carepo, A. Panplona, R. Franco, I. Moura, J. J. G. Moura and B. M. Hoffman, *J. Am. Chem. Soc.*, 1997, **119**, 9291–9292.
26 (*a*) Y. Montet, P. Amara, A. Volbeda, X. Vernede, E. C. Hatchikian, M. J. Field, M. Frey and J. C. Fontecilla-Camps, *Nat. Struct. Biol.*, 1997, **4**, 523–526; (*b*) Y. Montet, Thesis, Université Joseph Fourier, Grenoble, 1998.
27 H. Ogata, Y. Mizoguchi, N. Mizuno, K. Miki, S. Adachi, N. Yasuoka, T. Yagi, O. Yamauchi, S. Hirota and Y. Higuchi, *J. Am. Chem. Soc.*, 2002, **124**, 11628–11635.
28 Y. Higuchi, T. Yagi and N. Yasuoka, *Structure*, 1997, **5**, 1671–1680.
29 (*a*) A. E. Przybyla, J. Robbins, N. Menon and H. D. J. Peck, *FEMS Microbiol. Rev.*, 1992, **88**, 109–136; (*b*) C. Massanz and B. Friedrich, *Biochemistry*, 1999, **38**, 14330–14337.
30 M. Rousset, V. Magro, N. Forget, B. Guigliarelli, J. P. Belaich and E. C. Hatchikian, *J. Bacteriol.*, 1998, **180**, 4982–4986.
31 M. Rousset, Y. Montet, B. Guigliarelli, N. Forget, M. Asso, P. Bertrand, J. C. Fontecilla-Camps and E. C. Hatchikian, *Proc. Natl. Acad. Sci. USA*, 1998, **95**, 11625–11630.
32 A. Volbeda, Y. Montet, X. Vernède, E. C. Hatchikian and J. C. Fontecilla-Camps, *Int. J. Hydrogen Energy*, 2002, **27**, 1449–1461.
33 A. L. De Lacey, V. M. Fernandez, M. Rousset, C. Cavazza and E. C. Hatchikian, *J. Biol. Inorg. Chem.*, 2003, **8**, 129–134.
34 E. Garcin, X. Vernede, E. C. Hatchikian, A. Volbeda, M. Frey and J. C. Fontecilla-Camps, *Struct. Fold Des.*, 1999, **7**, 557–566.
35 Y. Higuchi, H. Ogata, K. Miki, N. Yasuoka and T. Yagi, *Struct. Fold Des.*, 1999, **7**, 549–556.
36 J. C. Fontecilla-Camps and S. W. Ragsdale, *Adv. Inorg. Chem.*, 1999, **47**, 283–333.
37 P. Amara, A. Volbeda, J. C. Fontecilla-Camps and M. Field, *J. Am. Chem. Soc.*, 1999, **121**, 4468–4477.
38 M. W. Adams, *Biochim. Biophys. Acta*, 1990, **1020**, 115–145.
39 A. J. Pierik, M. Hulstein, W. R. Hagen and S. P. Albracht, *Eur. J. Biochem.*, 1998, **258**, 572–578.
40 (*a*) J. W. Peters, W. N. Lanzilotta, B. J. Lemon and L. C. Seefeldt, *Science*, 1998, **282**, 1853–1858; (*b*) Y. Nicolet, C. Piras, P. Legrand, C. E. Hatchikian and J. C. Fontecilla-Camps, *Struct. Fold Des.*, 1999, **7**, 13–23; (*c*) Y. Nicolet, B. J. Lemon, J. C. Fontecilla-Camps and J. W. Peters, *Trends Biochem. Sci.*, 2000, **25**, 138–143.
41 Z. Chen, B. J. Lemon, S. Huang, D. J. Swartz, J. W. Peters and K. A. Bagley, *Biochemistry*, 2002, **41**, 2036–2043.
42 Y. Nicolet, A. L. de Lacey, X. Vernède, V. M. Fernandez, E. C. Hatchikian and J. C. Fontecilla-Camps, *J. Am. Chem. Soc.*, 2001, **123**, 1596–1601.
43 (*a*) L. Pieulle, V. Magro and E. C. Hatchikian, *J. Bacteriol.*, 1997, **179**, 5684–5692; (*b*) E. Chabrière, M. H. Charon, A. Volbeda, L. Pieulle, E. C. Hatchikian and J. C. Fontecilla-Camps, *Nat. Struct. Biol.*, 1999, **6**, 182–190.
44 P. M. Matias, C. M. Soares, L. M. Saraiva, R. Coelho, J. Morais, J. Le Gall and M. A. Carrondo, *J. Biol. Inorg. Chem.*, 2001, **6**, 63–81.
45 (*a*) S. Niu, L. M. Thomson and M. B. Hall, *J. Am. Chem. Soc.*, 1999, **121**, 4000–4007; (*b*) S. Niu and M. B. Hall, *Inorg. Chem.*, 2001, **40**, 6201–6203.
46 J. M. Coremans, J. W. van der Zwaan and S. P. Albracht, *Biochim. Biophys. Acta*, 1992, **1119**, 157–168.
47 A. Melis and T. Happe, *Plant Physiol.*, 2001, **127**, 740–748.
48 C. Leger, A. K. Jones, W. Roseboom, S. P. Albracht and F. A. Armstrong, *Biochemistry*, 2002, **41**, 15736–15746.
49 D. J. Berger, *Science*, 1999, **286**, 49.
50 (*a*) I. P. Georgakaki, M. L. Miller and M. Y. Darensbourg, *Inorg. Chem.*, 2003, **42**, 2489–94; (*b*) G. Musie, P. J. Farmer, T. Tuntulani, J. H. Reibenspies and Y. M. Darensbourg, *Inorg. Chem.*, 1996, **35**, 2176–83; (*c*) F. Gloaguen, J. D. Lawrence, T. B. Rauchfuss, M. Benard and M. M. Rohmer, *Inorg. Chem.*, 2002, **41**, 6573–82; (*d*) S. George, Z. Cui, M. Razavet and C. J. Pickett, *Chemistry*, 2002, **8**, 4037–46.
51 (*a*) K. K. Surerus, M. Chen, J. W. van der Zwaan, F. M. Rusnak, M. Kolk, E. C. Duin, S. P. Albracht and E. Munck, *Biochemistry*, 1994, **33**, 4980–4993; (*b*) M. Carepo, D. L. Tierney, C. D. Brondino, T. C. Yang, A. Pamplona, J. Telser, I. Moura, J. J. Moura and B. M. Hoffman, *J. Am. Chem. Soc.*, 2002, **124**, 281–286.
52 (*a*) O. Trofanchuk, M. Stein, C. Gessner, F. Lendzian, Y. Higuchi and W. Lubitz, *J. Biol. Inorg. Chem.*, 2000, **5**, 36–44; (*b*) S. Foerster, M. Stein, M. Brecht, H. Ogata, Y. Higuchi and W. J. Lubitz, *J. Am. Chem. Soc.*, 2003, **125**, 83–93.
53 (*a*) M. Stein and W. Lubitz, *Curr. Opin. Chem. Biol.*, 2002, **6**, 243–249; (*b*) C. Stadler, A. L. de Lacey, Y. Montet, A. Volbeda, J. C. Fontecilla-Camps, J. C. Conesa and V. M. Fernandez, *Inorg. Chem.*, 2002, **41**, 4424–34.
54 (*a*) M. Blokesch, A. Paschos, E. Theodoratou, A. Bauer, M. Hube, S. Huth and A. Bock, *Biochem. Soc. Trans.*, 2002, **30**, 674–680; (*b*) S. Reissmann, E. Hochleitner, H. Wang, A. Paschos, F. Lottspeich, R. S. Glass and A. Bock, *Science*, 2003, **299**, 1067–1070.